

ELECTROWEAK MEASUREMENTS IN THE FORWARD REGION AT THE LHCb*

W.C. ZHANG

on behalf of the LHCb Collaboration

School of Physics, University College Dublin, Dublin, Ireland

(Received January 25, 2013)

W , Z and low mass Drell–Yan production cross sections in proton–proton collisions at $\sqrt{s} = 7$ TeV have been measured with $W \rightarrow \mu\nu_\mu$, $Z \rightarrow \mu\mu$, $Z \rightarrow ee$, $Z \rightarrow \tau\tau$ and $\gamma^* \rightarrow \mu\mu$ channels in the LHCb detector. The cross section results are consistent with theoretical predictions calculated at next-to-next-to-leading order (NNLO) with different proton parton distribution functions (PDFs).

DOI:10.5506/APhysPolBSupp.6.635

PACS numbers: 13.60.Hb

1. Introduction

LHCb [1] is a single arm forward spectrometer specially designed to study b -physics. It covers the pseudo-rapidity, η , in the range of $2.0 < \eta < 5.0$. Of this, $2.0 < \eta < 2.5$ is common to ATLAS and CMS while $2.5 < \eta < 5.0$ is unique to LHCb. Thus, LHCb provides complementary measurements of electroweak physics to those performed by ATLAS and CMS. Here, we report on the cross section results for W , Z and low mass Drell–Yan production in the LHCb with approximately 37 pb^{-1} of data recorded in 2010 and 1 fb^{-1} of data recorded in 2011 at $\sqrt{s} = 7$ TeV.

W , Z and low mass Drell–Yan production cross section measurements provide an important test of the Standard Model. The uncertainty on NNLO predictions is dominated by PDF uncertainties. The PDF uncertainties change with boson rapidity [2]. In the kinematic region, where the uncertainty is low, electroweak measurements can test the Standard Model to a precision of 1%. In the kinematic region, where the uncertainty is high, a precise electroweak measurement in LHCb can be used to constrain PDFs.

* Presented at the International Symposium on Multiparticle Dynamics, Kielce, Poland, September 17–21, 2012.

2. Event selection

The $W \rightarrow \mu\nu_\mu$ cross section [3] is measured in approximately 37 pb^{-1} of data collected in 2010 with a single high transverse momentum (p_T) muon trigger. $W \rightarrow \mu\nu_\mu$ candidates are selected by requiring a well reconstructed muon with $p_T^\mu > 20 \text{ GeV}/c$ and $2.0 < \eta^\mu < 4.5$. In order to suppress heavy flavour and pion or kaon decay-in-flight backgrounds, the muon candidate is isolated by requiring the summed p_T of all charged tracks and identified photons inside a cone of radius around the muon, $R = \sqrt{\Delta\eta^2 + \Delta\phi^2} = 0.5$, to be smaller than $2 \text{ GeV}/c$. Heavy flavour is further suppressed by requiring the muon unbiased impact parameter to be less than $40\mu\text{m}$. Punch-through pions or kaons are further suppressed by requiring the relative energy, $(E_{\text{ECAL}} + E_{\text{HCAL}})/pc$, associated with the muon candidate deposit in the electromagnetic calorimeter (ECAL) and hadronic calorimeter (HCAL) be less than 0.04. $Z \rightarrow \mu\mu$ background is suppressed by requiring no extra muons in the event with $p_T > 2 \text{ GeV}/c$. 14660 W^+ and 11618 W^- candidates are selected with these requirements. The signal yield is determined by fitting the p_T spectrum of μ^+ and μ^- in data to templates representing signal and backgrounds. Figure 1(a) shows the fit result. In this figure, data are shown as points with error bars. The $W \rightarrow \tau\nu$, $Z \rightarrow \mu\mu$ and $Z \rightarrow \tau\tau$ background shapes are taken from simulation while their normalizations are determined from data. The heavy flavour background shape is taken from data with an anti-impact parameter cut while its normalization is taken from data. The signal and decay-in-flight templates are free to vary in the fit. After the fit, the purity for W^+ sample is 80% while for W^- sample it is 79%.

The $Z \rightarrow \mu\mu$ cross section [3] is measured in approximately 37 pb^{-1} of data collected in 2010 by a single high p_T muon trigger. $Z \rightarrow \mu\mu$ candidates are selected by requiring two well reconstructed muons with $p_T^\mu > 20 \text{ GeV}/c$ and $2.0 < \eta^\mu < 4.5$. The dimuon invariant mass must be in the range of $60 < M_{\mu\mu} < 120 \text{ GeV}/c^2$. 1966 $Z \rightarrow \mu\mu$ candidates are selected with these requirements. Figure 1(b) shows the dimuon invariant mass spectrum of the selected candidates. The mass spectrum is fitted with a crystal ball function (solid/red curve) modelling Z peak plus an exponential function (dashed/blue line) modelling the off-resonance Drell–Yan production and the small background contributions which mainly come from heavy flavour decays. The fitted mass is $90.7 \pm 0.1 \text{ GeV}/c^2$ and the width is $3.0 \pm 0.1 \text{ GeV}/c^2$.

The $Z \rightarrow ee$ cross section [4] is measured in approximately 945 pb^{-1} of data collected in 2011 by a single high p_T electron trigger. $Z \rightarrow ee$ candidates are selected by requiring two well reconstructed electrons with $p_T^e > 20 \text{ GeV}/c$ and $2.0 < \eta^e < 4.5$. The dielectron invariant mass must be greater than $40 \text{ GeV}/c^2$. In order to identify electrons, the relative energy in the ECAL (HCAL) is greater (smaller) than 0.1 (0.05), and the energy in the

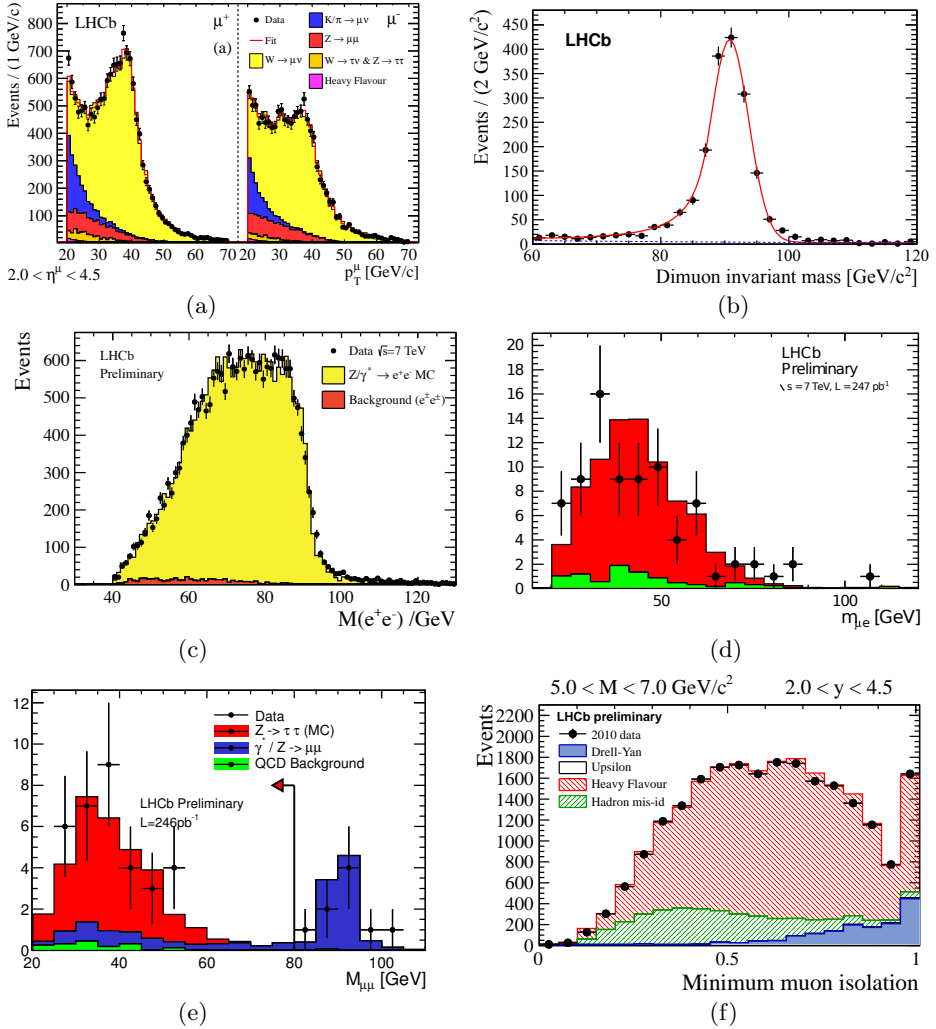


Fig. 1. (a) $W \rightarrow \mu\nu_\mu$ p_T distributions of μ^+ (left) and μ^- (right) in the range of $2.0 < \eta < 4.5$. (b) $Z \rightarrow \mu\mu$ dimuon invariant mass spectrum. (c) $Z \rightarrow ee$ dielectron invariant mass spectrum. (d) and (e) Dilepton mass spectrum for $Z \rightarrow \tau\tau$ in the μe and $\mu\mu$ channels separately. (f) Drell-Yan minimum muon isolation distribution in the mass range of $5.0 < M_{\mu\mu} < 7.0$ GeV/c².

preshower detector associated with the particle is greater than 50 MeV/c². 21526 $Z \rightarrow ee$ candidates are selected with these requirements. Figure 1 (c) shows the dielectron mass spectrum of the selected candidates. In the plot, the signal sample is taken from simulation. The main background is from pion or kaon mis-identification and is estimated from the same sign events in data. Its contribution is 473 ± 22 events.

$Z \rightarrow \tau\tau$ cross section [5] is measured in 248 pb⁻¹ of data collected in 2010 and 2011. One tau is identified by its decay to a muon and neutrinos; the other is identified by its decay to an electron or a muon and neutrinos. $Z \rightarrow \tau\tau$ candidates are selected by requiring one muon with $p_{\text{T}}^{\mu} > 20$ GeV/ c and $2.0 < \eta^{\mu} < 4.5$ and another muon or electron with $p_{\text{T}}^{\mu/e} > 5$ GeV/ c and $2.0 < \eta^{\mu/e} < 4.5$. The first lepton fires the trigger. Pion or kaon punch-through background is suppressed by requiring the relative energy in ECAL and HCAL to be less than 0.2. $Z/\gamma^* \rightarrow \mu\mu$ background in the $\mu\mu$ final state is suppressed by requiring the p_{T} balance between the two muons, $p_{\text{T}}^{\text{balance}} = (p_{\text{T}}^{(1)} - p_{\text{T}}^{(2)}) / (p_{\text{T}}^{(1)} + p_{\text{T}}^{(2)})$, where the superscript labels each μ , to be greater than 0.2. $Z/\gamma^* \rightarrow \mu\mu$ is further suppressed by requiring the significance of the summed signed muon impact parameter to be greater than 4. Background from pion or kaon mis-identification for both μe and $\mu\mu$ final states is suppressed by requiring the variable, $I^{\text{lepton}} = (p^{\text{lepton}} - \sum_i p_i^{\text{track}}) / (p^{\text{lepton}} + \sum_i p_i^{\text{track}})$, where the sum extends over all charged tracks inside a cone, to be greater than 0.8. Other electroweak backgrounds are suppressed by requiring the difference between the azimuthal angles of the leptons, $\Delta\phi$, to be greater than 2.7 radians. 81 (33) candidates are selected in μe ($\mu\mu$) final states. Figure 1 (d), (e) shows the dilepton mass spectrum for the selected candidates in μe ($\mu\mu$) final states. In both plots, the signal template is taken from simulation. For $\mu\mu$ (μe) final states it is estimated that 1.6 ± 1.3 (9.5 ± 3.0) events arise from QCD, 5.5 ± 1.8 (0) events arise from Drell–Yan.

The Drell–Yan cross section [6] is measured in 37 pb⁻¹ of data collected in 2010 by a dimuon trigger. Drell–Yan candidates are selected by requiring two well reconstructed muons with $p^{\mu} > 10$ GeV/ c and $2.0 < \eta^{\mu} < 4.5$. The dimuon mass must lie within the range of $5 < M_{\mu\mu} < 120$ GeV/ c^2 . For $M_{\mu\mu} < 40$ GeV/ c^2 ($M_{\mu\mu} > 40$ GeV/ c^2), the muon p_{T} must be greater than 3 GeV/ c (15 GeV/ c). The signal yield is obtained by fitting the minimum muon isolation distribution of the two muons in data to templates representing the signal and backgrounds. This is defined as the minimum fraction of μ -jet p_{T} carried by the two muons. The μ -jet is defined as the jet which contains the muon. It is reconstructed with the anti- k_t algorithm with the size $R = \sqrt{\Delta\eta_{ij}^2 + \Delta\phi_{ij}^2} = 0.5$. Here $\Delta\eta_{ij}$ and $\Delta\phi_{ij}$ give the separation of two particles in the jet in η and ϕ . The fit is performed in 9 mass bins and in 5 rapidity bins with 2 mass regions. Figure 1 (f) shows the fit result in one mass bin within the whole rapidity range. In this plot, the signal template is taken from simulation. The heavy flavour background shape is taken from data with impact parameter cut and it is free to vary in the fit. The pion or kaon mis-identification background shape is taken from data and it is free to vary in the fit. The Υ background shape is taken from simulation while its normalization is determined from data. The Drell–Yan signal purity is about 7% in the low mass range and is increased to 100% in the high mass range.

3. Cross section measurement

The cross sections for W , Z and low mass Drell–Yan production are derived from the product of the number of selected events and the sample purity divided by the product of integrated luminosity and total efficiency. The cross section is corrected for the final state radiation to allow accurate comparison with theoretical predictions. The total efficiency for selecting signal events is the product of: an acceptance factor, describing the proportion of events that are reconstructed inside a given kinematic region; an identification efficiency, describing the probability of identifying tracks as leptons; a trigger efficiency, describing the probability of triggering on such offline signal events; a tracking efficiency, describing the probability of reconstructing the leptons produced in signal sample as tracks; a selection efficiency, describing the probability of the leptons passing additional selection cuts. The muon (electron) identification, trigger and tracking efficiencies are determined from $Z \rightarrow \mu\mu$ ($Z \rightarrow ee$) data sample using a tag-and-probe method. In this method, one μ (e) is marked as tag and is well identified and fires the μ (e) trigger, the other μ (e) or a track candidate marked as probe is tested to see how often it fired the μ (e) trigger, is identified as a μ (e) or has a track associated to it.

4. Results

Figure 2(a) shows the $W \rightarrow \mu\nu_\mu$ differential cross section as a function of η^μ . Figure 2(b) shows the total cross sections for $Z \rightarrow \mu\mu$, $Z \rightarrow ee$ and $Z \rightarrow \tau\tau$. The cross section results for Z production with $\mu\mu$, ee and $\tau\tau$ channels are consistent and confirm lepton universality. Figure 2(c) shows the Drell–Yan differential cross section as a function of dimuon invariant mass. In this plot, the shaded vertical band corresponds to the mass region of Υ which is not included in the measurement. Figure 2(d) shows the Drell–Yan differential cross section as a function of dimuon rapidity. In these plots, dark shaded bands show the statistic uncertainties and light hatched bands show the total uncertainties by adding the statistic and systematic uncertainties in quadrature. The systematic uncertainties arise from background models, efficiency determination, final state radiation treatment and integrated luminosity error. For the $W \rightarrow \mu\nu_\mu$ cross section, the dominant systematic uncertainty is from the luminosity measurement. For the $Z \rightarrow \mu\mu$ cross section, the dominant systematic uncertainty is from efficiency determinations and is about 4%. For the $Z \rightarrow ee$ cross section, the dominant systematic uncertainty is from efficiency determinations and varies with the Z boson rapidity. For the $Z \rightarrow \tau\tau$ cross section, the dominant systematic uncertainty is from efficiency determinations and is 10% (11%) in μe ($\mu\mu$) channel. The leading systematic uncertainty for the Drell–Yan production cross section is from the shape of the heavy flavour template. This systematic uncertainty in the lowest mass bin is 24%, dropping to below 1%

for masses larger than $20 \text{ GeV}/c^2$. Data measurements are consistent with NNLO (NLO) theoretical predictions with a variety of PDF sets.

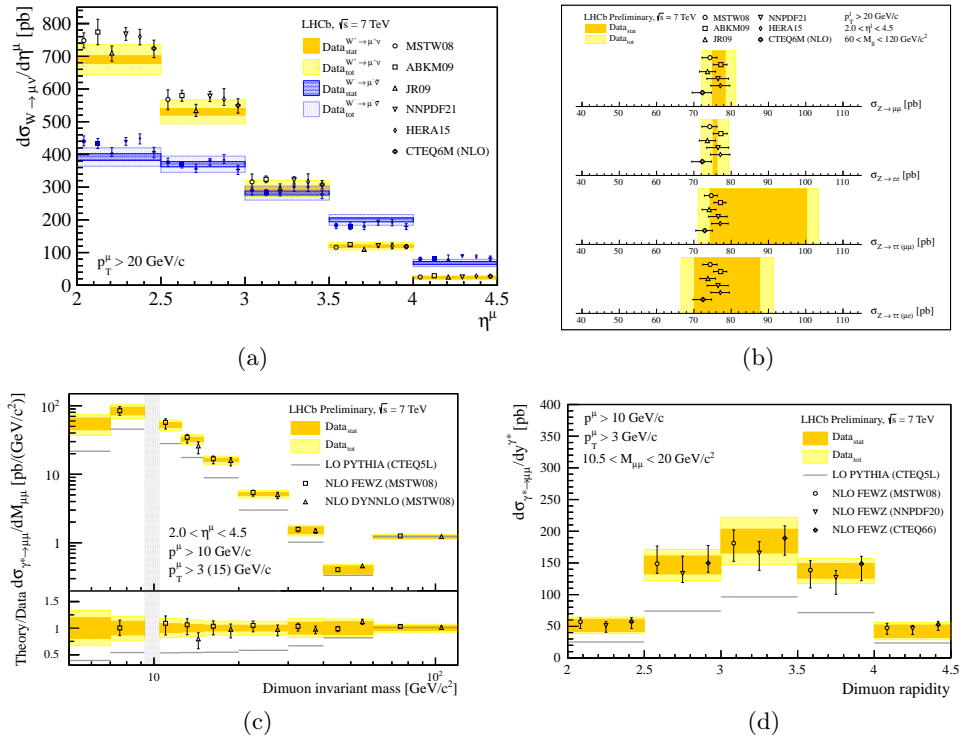


Fig. 2. (a) $W \rightarrow \mu\nu_\mu$ differential cross section as a function of η^μ . The light grey/yellow (dark grey/blue) band is for $W^+(W^-)$. (b) Total cross section for $Z \rightarrow \mu\mu$, $Z \rightarrow ee$ and $Z \rightarrow \tau\tau$. (c) Drell-Yan differential cross section as a function of $M_{\mu\mu}$. (d) Drell-Yan differential cross section as a function of dimuon rapidity.

REFERENCES

- [1] A. Augusto *et al.* [LHCb Collaboration], *JINST* **3**, S08005 (2008).
- [2] A.D. Martin *et al.*, *Eur. Phys. J.* **C63**, 189 (2009).
- [3] R. Aaij *et al.* [LHCb Collaboration], *J. High Energy Phys.* **06**, 058 (2012).
- [4] R. Aaij *et al.* [LHCb Collaboration], LHCb-CONF-2012-011(2012).
- [5] R. Aaij *et al.* [LHCb Collaboration], LHCb-CONF-2011-041(2011).
- [6] R. Aaij *et al.* [LHCb Collaboration], LHCb-CONF-2012-013(2012).